REIIBP promotes TLR7-BTK-IL6 pro-inflammatory response through histone H3 lysine methylation in t(4;14) myelomagenesis

Phyllis S.Y. Chong (mdcsyp@nus.edu.sg)
National University of Singapore
Jing Yuan Chooi
National University of Singapore
Sze Lynn Julia Lim
National University of Singapore
Tae-Hoon Chung
Cancer Science Institute of Singapore
Sabrina Hui Min Toh
Cancer Science Institute of Singapore
Kalpnaa Balan
Cancer Science Institute of Singapore
Muhamad Irfan Bin Azaman
National University of Singapore
Zhengwei Wu
Genome Institute of Singapore, Agency for Science, Technology and Research (A*STAR)
Chng Wee-Joo
National University Cancer institute of Singapore, The National University Health System (NUHS)

Research Article

Keywords: MMSET, REIIBP, Histone Methyltransferase, EZH2, microRNAs, TLR7, BTK, Bortezomib, Ibrutinib, Multiple Myeloma

Posted Date: April 13th, 2022

DOI: https://doi.org/10.21203/rs.3.rs-1539915/v1

Abstract

Background

Recurrent chromosomal translocations are central to the pathogenesis of Multiple Myeloma (MM), and the t(4;14) translocation is an adverse prognostic factor found in approximately 15% of MM patients. REIIBP is a t(4;14)-deregulated histone methyltransferase arising from alternative promoter usage within the MMSET locus. The role of this short isoform in t(4;14) myelomagenesis is poorly understood.

Methods

RPMI8266 was transfected with REIIBP vector to create stable isogenic cells using puromycin selection, and the oncogenic and histone methyltransferase activities were evaluated by RT-qPCR, immunoblotting, viability and colony-forming assays. Microarray and ChIP-sequencing were used to identify REIIBP targets, followed by genetic and biochemical inhibition to determine the underlying mechanisms *in vitro* and *in vivo*. Clinical relevance was validated with CoMMpass dataset.

Results

Despite sharing identical sequence with the C-terminus of *MMSET*, we found that REIIBP displayed distinct expression pattern with other MMSET breakpoint variants and gene products of the t(4;14) locus. Additionally, the expression of REIIBP can be regulated through microRNAs by another histone methyltransferase, EZH2 in a Dicer-dependent manner. Stable overexpression of REIIBP in the t(4;14)-negative RPMI8226 promoted oncogenic phenotypes and predominantly catalyzes the repressive H3K27me3 and active H3K4me3 histone modifications. Identification of differentially-regulated genes through microarray and correlation with H3K4me3/H3K27me3 ChIP-sequencing revealed that Toll-like receptor 7 (TLR7) and Bruton's tyrosine kinase (BTK) are targets of REIIBP. Importantly, this led to a B-cell receptor (BCR)-independent activation of BTK and NF-κB effector signaling in t(4;14) myeloma cells. As myeloma cells do not express BCR, the re-activation of BTK signaling by TLR7 was functionally validated, conferring bortezomib resistance through the dysregulation of pro-inflammatory cytokine expression such as IL-6 and IL-27. Furthermore, comparison of BTK expression and dependency scores across lineages revealed that BTK is an important target in multiple myeloma, and correlated with REIIBP expression in the CoMMpass dataset. t(4;14)-translocated cells were amenable to BTK targeting using Ibrutinib, improving bortezomib response in myeloma cells and mice engrafted with RPMI8226-REIIBP tumors.

Conclusion

Altogether, our results provided a rationale for the blockade of REIIBP in t(4;14) cells through combining proteasome and BTK inhibitors as a therapeutic strategy for further clinical evaluation.

Background

Multiple Myeloma (MM) is a neoplasm of plasma cells characterized by the uncontrolled proliferation of abnormal plasma cells in the bone marrow that is incapable of producing functional antibodies[1]. Current treatment regime involves single or combination of novel drug classes such as proteasome inhibitors (bortezomib), immunomodulatory drugs (lenalidomide) and monoclonal antibodies (daratumumab), which have significantly improved survival outcomes in patients[2–4]. However, this disease still represents an important clinical challenge as it mainly affects the elderly population and frequent development of drug resistance subsequent to initial treatment response. MM can be broadly divided into hyperdiploid and non-hyperdiploid subtypes, with the non-hyperdiploid cases identified by recurrent IgG translocations such as t(4;14)(p16;q32) and t(11;14)(q13;q32) in ~ 15% of MM patients respectively[5,6]. Such recurrent chromosomal translocations are central to the pathogenesis of MM and predicts the treatment response and clinical outcome of the patient. Patients with t(4;14) translocation, which displays a dysregulation of the *MMSET* locus and its alternatively spliced variants, has one of the worst prognosis when compared to other biological subgroups, but represents an intermediate-risk group given its response towards bortezomib[7,8].

We and others have sought to study the function of the protein products arising from this *MMSET* gene, which includes the full-length isoform MMSET II, and the shorter isoforms MMSET I and REIIBP[9–19]. MMSET II contains 1365 amino acids, and harbors conserved motifs such as PWWP domain, PHD-type zinc fingers and HMG box which are typically found in proteins with chromatin-binding ability and recognition of histone marks. The C-terminal region resides a functional and catalytic SET domain, which is essential for the oncogenic activities of MMSET II. *In vitro* and *in vivo* histone methyltransferase assays demonstrated that the primary activity of MMSET II is H3K36 dimethylation, which leads to a global gene activation reprogramming that drives myelomagenesis[11]. Other histone modifications modulated by MMSET II includes H4K20 and H3K27 methylation, as well as H3 acetylation[12–14]. Through its histone modifying activities, MMSET II promoted cancer phenotypes such as increased cell proliferation, clonogenicity, adhesion to bone marrow stroma and tumorigenesis[11,15–17]. MMSET I is identical to the N-terminus region of MMSET II spanning 647 amino acids. Despite lacking the SET domain, it regulates gene expression through binding to the promoter of target genes such as *GLO1*, and truncation studies indicated that the HMG-box at the C-terminus of MMSET I was important for this function[18]. On the other hand, the role of REIIBP, which is overexpressed independent of *MMSET* breakpoint clusters, is poorly understood [9,10]. This transcript arises from the intron 9 of the *MMSET* locus and is identical to the C-terminus of MMSET II spanning 584 amino acids, retaining the SET domain[19]. The subcellular localization of REIIBP is found in the cytoplasm and nucleoli, which differs from MMSET I and II that reside in the nucleus[9]. Hence, it is likely that REIIBP have differential histone methylation targets as well as novel functions that are not fully elucidated. In this study, we generated a stable cell

line that overexpresses REIIBP to perform an unbiased study of the histone methylation and regulatory activities of REIIBP.

Methods

Cell lines, plasmids and reagents

Human myeloma cell lines (RPMI8226, KMS11, KMS34, KMS18, H929, OPM2, KMS12BM, U266) and K562 were cultured in RPMI-1640 medium and 293T cells were cultured in DMEM supplemented with 10% FBS and 10 mg/mL penicillin/streptomycin, and incubated at 37^0C with 5% CO_2. Cell lines were authenticated (National University of Singapore, Singapore) and tested to be *Mycoplasma*-free (Lonza, Switzerland). Full-length MMSET II, MMSET I and REIIBP were cloned as previously described[11,18], and antibodies and real-time primers used to differentiate MMSET isoforms were listed in Supplementary Methods. Dicer and TLR7 shRNAs were constructed in pRP(shRNA)-EGFP-U6 vector by VectorBuilder (USA). Precursor microRNAs miR-26a, miR-31, and miR-203 were cloned in pRP[ncRNA]-Puro-CMV vector by VectorBuilder (USA). EZH2 siRNA was purchased from Thermo Fisher Scientific ((USA); EPZ-6438 and GSK-126 were purchased from Selleck Chemicals (USA). Ibrutinib, Bortezomib and Loxoribine were purchased from Santa Cruz (USA).

In vitro histone methyltransferase activity assay

Histone H3 tri-methyl K27 and K4 quantification kits were purchased from Abcam and performed as per manufacturer's instructions. 0, 2, 5, 10 or 20 µg of nuclear extracts (Thermo Fisher Scientific) were added to biotinylated substrate (unmethylated histone peptide) and anti-H3K27me3 or anti-H3K4me3 antibody is used for capture and readings taken at absorbance 450 nm with a microplate reader (Tecan). S-adenosylmethionine (SAM) methyltransferase assay is performed using 1µM SAM as a methyl-group donor to modify 2µg of H3 substrate by 2µg REIIBP in a reaction buffer previously described[20] at 30°C for 2 hours. Proteins were resolved on 15% SDS-PAGE and probed with indicated antibodies.

ChIP sequencing

ChIP sequencing was performed on isogenic cell lines RPMI8226-Vcon and RPMI8226-REIIBP (20 million cells each) using reagents obtained from Cell Signaling Technology (SimpleChIP® Enzymatic Chromatin IP Kit) according to manufacturer's protocol. Monoclonal antibodies used for ChIP were anti-H3K27me3 (CST, #9733) and anti-H3K4me3 (CST, #9751). DNA were extracted with MinElute PCR Purification Kit (Qiagen). The purified DNA was used for ChIP-seq library preparation. The library was constructed by Novogene Corporation (Beijing, China). Subsequently, pair-end sequencing of sample was performed on Illumina platform (Illumina, CA, USA). Library quality was assessed on the Agilent Bioanalyzer 2100 system. Clean reads were aligned to the reference genome using BWA mem (v 0.7.12). After mapping reads to the reference genome, we used the MACS2 (version 2.1.0) peak calling software to identify regions of IP enrichment over background. A q-value threshold of 0.05 was used for all data sets. The

reference genome ID used was ensembl_homo_sapiens_grch38_p12_gca_000001405_27 and the ChIP-seq peaks were visualized using Integrative Genomics Viewer (IGV, Broad Institute).

Interleukin-6 in cell culture supernatant

Myeloma cells were seeded in a 10 cm dish in 10 mL of medium at a density of 1×10^6/ml. After 24h, cells were seeded in serum free RPMI. Supernatant was collected after 24h culture in serum free RPMI and concentrated in Amicon Ultra-0.5 Centrifugal Filter Unit (3K filter unit) as per manufacturer's instructions. After centrifugation, both supernatants collected in filter units and flow through were used for detection of protein by Western Blotting.

In vivo xenograft study

To generate REIIBP xenograft model, RPMI8226-REIIBP stable cells (5×10^6) were suspended in 0.1 mL PBS and subcutaneously injected into the flanks of NOD/SCID female mice (6 weeks old, InVivos). Tumor growth was monitored using calipers every 3 days until a volume of 150mm^3 [calculated as length x width (2)/2] is reached, which developed between 2-3 weeks, and randomized into four groups: DMSO (1% final concentration), Ibrutinib (15mg/kg), Bortezomib (0.4mg/kg) and combination (n=5 mice/group). Treatment was performed every 2 days via intraperitoneal (I.P) injection for 2 weeks. Tumors were harvested for weight analysis. The responsible use of animals was approved and in accordance to protocol by Institutional Animal Care and Use Committee (IACUC; National University of Singapore).

Statistical Analysis

All data were performed in biological replicates and values presented as the mean ± standard deviation. qRT-PCR assays were done in duplicates with three biological repeats; CTG viability assays were performed in sextuplicate with three biological repeats; apoptosis and cell cycle assays were performed in triplicates. Paired or unpaired student t-tests were used to compare significant differences between groups with Excel or GraphPad Prism 9. Correlation analyses were performed between REIIBP (ENST00000382888, transcript NSD2-203 of Enesmbl annotation) and BTK in CoMMpass dataset using Pearson correlation analysis. Survival analysis was performed using Kaplan–Meier method and assessed using the log-rank test in Excel. Using Wilcoxon's test, association between REIIBP expression and bortezomib response was determined in CoMMpass (IA13a version) drug treatment response data that had included bortezomib as a part of the regimen. The levels of significance were designated as follows: *, $P < 0.05$; **, $P < 0.01$; ***, $P < 0.001$.

Detailed description available in Supplementary Methods.

Results

REIIBP is expressed in t(4;14)$^+$ myeloma cells independent of other MMSET isoforms, *FGFR3* or *ACA11* expression and harbored oncogenic activity

To elucidate the biological role of REIIBP in myeloma, we first examined the endogenous expression of REIIBP in human myeloma cell lines (HMCLs). We optimized an antibody that recognizes the C-terminus region of MMSET and detected a band that corresponded to REIIBP at ~62kDa. Using a different N-terminus antibody, we probed for MMSET I and MMSET II. Consistent with previous reports, we detected the longest isoform of MMSET II in KMS11 and KMS34 cells, and these cells harbored the highest expression for MMSET I (Figure 1A). On the contrary, REIIBP expression was lower in KMS11 and KMS34, but abundantly expressed in other t(4;14)$^{+}$ cells, while the t(4;14)$^{-}$ cells showed little to null expression of REIIBP (Figure 1A). Interestingly, abrogating MMSET II led to an upregulation of REIIBP, in turn, overexpression of REIIBP downregulated MMSET II (Supplementary Figure 1A). Next, we compared REIIBP transcript levels against other gene products that were reported to be associated with t(4;14) locus, namely *FGFR3* and *ACA11*[9,21], but no clear correlation were observed (Figure 1B). Additionally, in t(4;14) negative cells, we could detect REIIBP mRNA which was not translated into REIIBP protein (Figure 1A and 1B), suggesting a post-transcriptional regulatory mechanism of REIIBP in myeloma cells. Another MM cell line frequently used to study MMSET isoforms is the TKO (translocation knockout) cells generated from the parental KMS11 with the exon 7 on t(4;14) translocated *MMSET II* allele deleted[16,22]. This results in almost undetectable protein levels of MMSET I and II, and TKO cells also lacked the protein expression of REIIBP (Figure 1C).

To examine the physiological functions of REIIBP, we engineered RPMI8226 to stably overexpress REIIBP given its low expression of all MMSET gene products (Figure 1D). In consideration of its proposed role as a histone methyltransferase, we first checked whether REIIBP could be found in the nucleus. Ectopically expressed and endogenous REIIBP were detected in both the nuclear and cytoplasmic compartments of the cell (Figure 1E). This contrasts with the exclusive expression of MMSET I and II in the nucleus. Compared to control (8226 V-Con), overexpression of REIIBP promoted myeloma cell growth in a short-term viability assay (Figure 1F) and a significant increase in soft agar clonogenic growth (Figure 1G). These were attributed to an increased cell-cycle progression (Figure 1H) with little effect on apoptosis (Supplementary Figure 1B). To exclude cell specific observations, we transiently overexpress REIIBP in two other t(4;14)$^{-}$ cells, KMS12BM and U266, where REIIBP similarly promoted cell viability (Supplementary Figure 1C). Altogether, REIIBP conferred growth and survival advantage to myeloma cells independent of other t(4;14) products.

REIIBP has histone methyltransferase activity centered on histone 3 lysine 27, lysine 4 and lysine 79 *in vitro*

Till date, whether the SET domain of REIIBP is enzymatically active and its substrate specificity remains unclear. To examine whether REIIBP has a direct effect on histone methylation, we performed an *in vitro* histone methyltransferase assay using the methyl donor S-adenosylmethionine (SAM), the substrate H3 and purified REIIBP (Figure 2A). After incubation, the methylated products were visualized by immunoblot. We first performed the assay using bacterial cell extracts[23] where we expressed a recombinant GST-tagged REIIBP, and detected a specific modification of H3K27me3 (Figure 2B). As

bacterially-purified enzymes might not be fully activated either because of absence of post-translational modifications or other mammalian complex proteins, we repeated with 293T-purified REIIBP. We confirmed a catalyzation of trimethylation on H3K27, additionally, we also detected modifications on H3K4 and H3K79 residues (Figure 2C). To exclude the possibility of contamination with other histone modifying enzymes, we probed for EZH2 that catalyzes H3K27me3[24] and H3K79 methyltransferase DOT1L[25], which were both undetected in the extracts (Figure 2C). We performed further validation by directly measuring the enzymatic activity of nuclear extracts from the isogenic cells in a H3K27 and H3K4 histone methyltransferase reaction, where increased activity could be seen with REIIBP overexpression (Figure 2D and 2E).

REIIBP has different preferences for histone 3 substrates from MMSET II *in vivo*

To complement the *in vitro* assay, we performed a series of *in vivo* immunoblot panel screening of histone methylation marks. REIIBP increased the global abundance of H3K4, H3K9, H3K27 and H3K79 trimethylation, with lesser effects on dimethylation (Figure 3A). To identify SET-dependent modifications, we transfected the cells with SET mutant R357Q, which saw an efficient abolishment of H3K4me3 and H3K27me3 histone marks (Figure 3B). We then reconstituted the expression of REIIBP in the KMS11-TKO cells, and observed a consistent increase in H3K27me3 and H3K4me3 modifications by REIIBP (Figure 3C). As a direct comparison of the catalytic activities among MMSET II, MMSET I and REIIBP, we overexpressed these proteins in RPMI8226 cells in parallel. We observed the most significant increase in H3K36me2 by MMSET II, which was consistent with previous report[11]. Conversely, H3K27me3 and H3K4me3 were increased by REIIBP, but not MMSET I and II (Figure 3D). The modifications by REIIBP on these histone marks were reproducible in two other myeloma cells, U266 and KMS12BM (Figure 3E). Collectively, our *in vitro* and *in vivo* histone methylation assays indicated a SET-dependent activity of REIIBP on H3K4 and H3K27 trimethylation.

EZH2 is an upstream regulator of REIIBP and mediated through microRNAs

EZH2 is a key H3K27me3 enzyme, and previous reports linked EZH2 upstream of MMSET II[13,26]. To define the relationship between REIIBP and EZH2, we first checked the expression of EZH2 in our isogenic cells. Similar levels of EZH2 suggested that the upregulation of H3K27me3 is unlikely attributed to a modulation of EZH2 levels (Figure 4A). Next, we overexpressed REIIBP in a K562-EZH2 null cell line ($EZH2^{\Delta/\Delta}$), which led to a restoration of H3K27me3 levels in the absence of EZH2 (Figure 4B). We further checked a panel of other histone methyltransferases and demethylases. Most were unchanged except for downregulation, and not upregulation, of H3K4 methyltransferases MLL4 and SMYD1 (Figure 4C). Overall, these data indicated that H3K27 and H3K4 trimethylation mediated by REIIBP were independent of other enzymes.

Next, we inhibited EZH2 via two different mechanisms, siRNA-mediated abrogation of EZH2 levels, and pharmacological inhibitors (EPZ-6438 and GSK-126) known to affect EZH2-mediated H3K27me3 but leave EZH2 levels unchanged[27]. Knockdown of EZH2 showed an almost complete abrogation of MMSET

II and H3K36me2, thus acting as a positive control in our system. Notably, REIIBP was also abrogated but not MMSET I, and REIIBP-associated H3K4me3 and H3K27me3 were reduced (Figure 4D). This indicated that EZH2 not only regulated MMSET II, but REIIBP as well. Treatment with EZH2 inhibitors (EZH2i) provided alternative insights as it reduced H3K27me3 levels in wild-type cells but not in REIIBP-overexpressing cells (Figure 4E). The residual H3K27me3 in EZH2i-treated REIIBP-overexpressing cells confirmed that REIIBP could modulate H3K27me3 levels that was not targetable by EZH2i. Here, EZH2i did not affect REIIBP levels and correspondingly, H3K4me3.

EZH2 regulated MMSET II expression level through microRNAs (miRNAs)[26]. Given the identical 3'UTR of MMSET II and REIIBP, this prompted us to determine whether REIIBP expression level is likewise regulated by miRNAs and the specific EZH2-repressed miRNAs that might be targeting REIIBP. In OPM2, depletion of Dicer using two independent shRNAs rescued the mRNA and protein levels of REIIBP (Figure 4F). There were other cell lines whereby Dicer knockdown led to a downregulation of EZH2, resulting in the depletion of REIIBP (Supplementary Figure 2), strengthening our hypothesis that EZH2 was upstream of REIIBP. Lastly, we overexpressed the three EZH2-regulated miRNAs that were previously reported to target the 3'UTR of MMSET gene[26], namely miR-26a, miR-31, and miR-203. These miRNAs resulted in the abrogation of both MMSET II and REIIBP levels (Figure 4G).

Gene Expression Profiling identified an upregulation of BTK and its putative upstream regulator TLR7 in REIIBP-overexpressing cells

To investigate transcriptional reprogramming by REIIBP, we performed gene expression profiling on our RPMI8226 isogenic cells (Figure 5A, Supplementary Table 1). We identified 365 downregulated and 256 upregulated genes upon REIIBP overexpression (Figure 5B). The differentially expressed genes (DEGs) were subjected to gene ontology analysis, and functional annotation clustering revealed an enrichment in processes such as immune response, cell growth regulation and metabolism (Figure 5C). To uncover potential targets that could drive REIIBP oncogenic phenotype, we selected five upregulated genes (*CYBB, TLR7, FAIM3, BTK, PDIA2*) and validated them using qRT-PCR in RPMI8226, KMS12BM and U266 cells (Figure 5D). Additionally, WB validation was further performed for Toll-like receptor 7 (TLR7) and Bruton's tyrosine kinase (BTK) (Figure 5E) as it was interesting that both BTK and its putative upstream regulator TLR7[28] were upregulated by REIIBP. BTK is involved in BCR signalling and activates NF-kB signalling pathway to promote B-cell survival[29]. Pharmacological inhibitors of BTK have shown single-agent efficacy in various B-cell malignancies such as chronic lymphocytic leukemia (CLL) and mantle cell lymphoma (MCL)[30-32], indicating the importance of BTK signaling. Cancer Cell Line Encyclopedia and DepMap portal (Broad Institute) comparison of the expression of BTK and BTK dependency scores across lineages revealed that BTK is also an important target in MM (Supplementary Figure 3A and 3B). For clinical relevance, we found that TLR7 expression was associated with overall survival (OS) in CoMMpass dataset, although BTK showed a less significant association with OS (Figure 5F). However, there was a positive correlation (r=0.401, p =0) between REIIBP and BTK expression specifically in MMSET group but not in the overall cohort (Figure 5G).

Altered distribution of H3K4me3 and H3K27me3 on TLR7 and BTK by REIIBP activates the BTK signaling axis

Next, we performed genome-wide mapping of H3K4me3 and H3K27me3 histone marks using ChIP-sequencing. At the global level, we observed an increased enrichment of H3K4me3 near the TSS in REIIBP-overexpressing cells, while H3K27me3 was higher near the TSS and lowers with distance away from TSS (Figure 6A). To establish whether TLR7 and BTK expression were associated with histone changes, we examined their representative gene tracks. Higher H3K4me3 signals were observed on both gene loci near the promoter region, with broad lower H3K27me3 distribution across the gene body, indicating transcriptionally active chromatin (Figure 6B). We further examined *CYBB*, *FAIM3* and *PDIA2*. *PDIA2* was the only gene that did not show the presence of H3K4me3 on the promoter of its gene locus between the isogenic samples (Supplementary Figure 4), suggesting that it might not be a direct target of REIIBP.

Given the increased expression of TLR7 and BTK by histone methylation, we next examined whether they are functionally required for REIIBP oncogenesis. We observed elevated levels of phospho-BTK and phospho-NFκB with reduction in the inhibitory molecule IκBα[33], indicating an activation of downstream BTK signaling pathway (Figure 6C). In the absence of BCR, we hypothesize that TLR7 may be the functional receptor in BTK activation. shRNA-mediated gene silencing of TLR7 significantly reduced both BTK and phospho-BTK (Figure 6D), while stimulation with a TLR7 agonist, loxoribine, phosphorylated BTK in myeloma cells in a dose- and time-dependent manner (Figure 6E). Hence, our results indicated that REIIBP-mediated TLR7 upregulation was required for a fully activated, phosphorylated BTK.

TLR7-BTK activation conferred bortezomib resistance through aberrant pro-inflammatory cytokine production and can be targeted using Ibrutinib

Bortezomib resistance is a clinical challenge in the treatment of MM. Our data indicated that REIIBP overexpression contributed to bortezomib insensitivity (Figure 7A). This insensitivity was reliant on TLR7 activation as induction of TLR7 with loxoribine could reproduce bortezomib resistance in a similar manner to REIIBP overexpression (Supplementary Figure 5A), even when loxoribine alone did not confer viability advantage (Supplementary Figure 5B and 5C). The contribution of REIIBP expression towards bortezomib-based treatment response was clinically validated with the MMRF CoMMpass dataset. REIIBP expression was highest in progressive disease (PD) compared with the others in a six-level description (Figure 7B). Notably, the differences in REIIBP expression was also pronounced in a two-level segregation of negative versus positive response groups (Figure 7C). To understand the underlying mechanism, we measured the levels of pro-inflammatory cytokines as previous studies suggested that BTK activation elicits a pro-inflammatory response to support myeloma cell survival and drug resistance[34]. Consequently, we found a significant dysregulation of cytokine gene expression, especially IL-6 upon REIIBP overexpression (Figure 7D), with increased secretion of IL-6 into the supernatant by the myeloma cells (Figure 7E).

Next, we examined whether BTK activation could give rise to a new vulnerability that can be therapeutically targeted using Ibrutinib, a first-in-class oral inhibitor of BTK[35-37]. t(4;14) myeloma cells with high levels of REIIBP such as OPM2, H929 and KMS18 were significantly inhibited as compared to t(4;14) cells harbouring lower REIIBP like KMS11 and KMS34, while t(4;14)-negative U266 was the most unresponsive to Ibrutinib (Figure 7F). This efficacy was confirmed in RPMI8226 with REIIBP overexpression, but not control cells (Supplementary Figure 6A-C), demonstrating that REIIBP expression segregates response towards Ibrutinib. Moreover, the inhibitory effects of Ibrutinib were potentiated when used in combination with Bortezomib as assessed by cell viability assay (Figure 7G), apoptosis (Figure 7H), and Western blotting of apoptotic markers (Figure 7I). *In vivo*, NSG mice engrafted with RPMI8226-REIIBP cells developed tumors and randomized treatment with Ibrutinib-Bortezomib combination demonstrated superior results to single drug or DMSO control groups (Figure 7J). These results collectively indicated that BTK is a good druggable target against REIIBP and is a promising candidate for Bortezomib combination.

Discussion

Alternative splicing events and promoter usage are major contributors to isoform diversity, giving rise to functionally different protein products from the same gene locus, a phenomenon common for oncogenes. *MMSET* is amongst the genes that has been demonstrated to produce multiple transcripts. However, the mechanism of how each transcript contributed to myeloma phenotype remains to be fully elucidated. In particular, little is known about the oncogenic function and therapeutic potential of targeting REIIBP, due to the inability to perform REIIBP knockdown studies owing to a significant amount of overlapping gene sequences with MMSET II, and the absence of an REIIBP specific antibody. To overcome these technical difficulties, we created a stable isogenic REIIBP cell line using RPMI-8226, which do not express all isoforms of MMSET. We elaborated on the molecular mechanism regulating REIIBP expression, which was not only driven by chromosomal rearrangement, but also EZH2-mediated microRNA gene silencing. Our findings corroborated a previous study that implicated EZH2 as an upstream regulator of MMSET II via its 3'UTR[26], which is identical between REIIBP and MMSET II. This supports the notion that most histone modifying enzymes do not work singly, but in a concerted effort to remodel the chromatin and alter transcription[38,39]. Here, we also uncovered a cooperative network consisting of various epigenetic regulators in t(4;14) MM.

One major finding is that despite homology between REIIBP and MMSET II, the most prominent histone methylation activity of REIIBP is distinct from MMSET II. REIIBP preferentially modifies H3K27me3 and H3K4me3, with slight effect on H3K36me2, the primary modification mediated by MMSET II. As the catalytic SET domain of REIIBP and MMSET II is identical, a reasonable interpretation will be a combination of contributing factors such as differences in its subcellular localization or protein interacting partners, both of which can be caused by the absence of N-terminus sequences in REIIBP. Our results also further emphasise the promiscuity of the SET domain, which is supported by other literature based on the observed catalytic activity of MMSET II[12–15,40–41]. Traditionally, EZH2 is the only known

histone methyltransferase that catalyzes H3K27me3. Hence, we considered the possibility that REIIBP might indirectly regulate H3K27me3 levels through EZH2 or H3K27 demethylase JMJD3; however, neither was misregulated by REIIBP. Through a series of in vitro and in vivo experiments, we showed that REIIBP may have intrinsic H3K27 methylation capabilities. The accumulation of H3K27me3 by REIIBP, which is associated with a closed chromatin state and transcriptional repression, was generally reflected in our microarray data where we saw more downregulated genes. H3K4me3 opposes the role of H3K27me3 by predominantly marking active promoters[42]. In a bivalent domain, the co-occurrence of these two histone marks has been reported in embryonic stem cells as a mechanism to poise developmental genes for timely activation[42]. However, we did not observe true bivalent promoters since H3K4me3 was found near the TSS, while H3K27me3 was broadly distributed throughout the intragenic region without domains being simultaneously marked.

It was within our expectations that we found little overlap of the differentially-regulated genes between REIIBP and MMSET II[43], given the differences in histone preferences between them. Here, we uncovered a novel mechanism of BTK activation that bypasses BCR by REIIBP. BTK is a critical component of BCR signaling and a potent B cell survival factor, but BCR is lost when B cell matures into plasma cells[44]. However, BTK is highly expressed in MM, and we found that upregulation of TLR7 by REIIBP could represent a novel, important mechanism of BTK reactivation. Moreover, TLR7 is not expressed in the plasma cells from healthy donors[45], making it possible to target cancer cells while sparing normal cells. We further reasoned that TLR- or BCR-mediated BTK activity could elicit differential downstream effects. Probing for all the downstream effectors of BTK signaling helped us to identify a NF-κB-driven production and secretion of a key pro-inflammatory cytokine IL-6. Myeloma cells are highly dependent on the bone marrow tumor microenvironment and especially IL-6 for growth and survival, and the elevated expression of IL-6 is deemed a contributing factor for drug resistance[46–48]. This was reflected in our analysis of the CoMMpass database demonstrating that patients who expressed high REIIBP levels had poorer response towards bortezomib as compared to those expressing lower REIIBP, even though patients with t(4;14) translocation are generally perceived to be responsive towards bortezomib treatment.This also rendered REIIBP-overexpressing cells highly dependent on BTK and targetability using Ibrutinib to improve bortezomib response.

Conclusion

In summary, we demonstrated that REIIBP is a functional histone methyltransferase in t(4;14) myeloma, and upregulation of TLR7 by REIIBP methylation is a novel mechanism to bypass BCR and activate BTK-NFκB-IL6 signalling. Our work thus identifies REIIBP as a relevant target in t(4;14) MM that leads to epigenetic reprogramming of myeloma cells, and propose REIIBP overexpression as a selection biomarker for ibrutinib in combination with bortezomib.

Declarations

Availability of data and materials

The ChIP-seq data from this study were submitted to NCBI GEO (http://www.ncbi.nlm.nih.gov/geo/) under accession number GSE198026. Microarray data is provided as Supplementary Table 1.

Acknowledgements

We thank Dr. Frank Eisenhaber for insightful discussions on HMT assays. We thank Dr. Reinhard Brunmeir for EZH2 siRNA, inhibitors and K562 EZH2$^{\Delta/\Delta}$ cells and advice on ChIP-seq analysis. We thank Dr. Xie Zhigang for his involvement in the conceptualization of the project. We thank Dr. Zhou Jianbiao for advice on the *in vivo* mouse work.

Funding

WJC is supported by NMRC Singapore Translational Research (STaR) Investigatorship. This research is partly supported by the National Research Foundation Singapore and the Singapore Ministry of Education under the Research Centers of Excellence initiative as well as the RNA Biology Center at the Cancer Science Institute of Singapore, NUS, as part of funding under the Singapore Ministry of Education's Tier 3 grants, grant number MOE2014-T3-1-006.

Authors' Contributions

P.S.Y.C and J.Y.C designed the study and performed the experiments, analysed and interpreted data, P.S.Y.C prepared the manuscript; P.S.Y.C and T.H.C did the bioinformatics analyses; L.S.L.J, M.I.B.A and Z.W did the in vitro work; S.H.M.T and K.B did the mouse work; W.J.C. initialized the study, provided study directions, and proofread and finalized the manuscript.

Consent for publication

All authors have agreed to publish this manuscript.

Competing Interest

The authors declare that they have no competing interests.

References

1. Palumbo A, Anderson K. Multiple myeloma. N Engl J Med. 2011; 364: 1046–1060
2. Lu, S., Wang, J. The resistance mechanisms of proteasome inhibitor bortezomib. Biomark Res 1, 13 (2013).
3. Quach H, Ritchie D, Stewart AK, et al. Mechanism of action of immunomodulatory drugs (IMiDS) in multiple myeloma. Leukemia. 2010;24(1):22–32.

4. Raedler LA. Darzalex (Daratumumab): First Anti-CD38 Monoclonal Antibody Approved for Patients with Relapsed Multiple Myeloma. Am Health Drug Benefits. 2016;9(Spec Feature):70-73.
5. Fonseca R, Bergsagel PL, Drach J, et al. International Myeloma Working Group molecular classification of multiple myeloma: spotlight review. Leukemia. 2009;23(12):2210–2221.
6. Chng WJ, Glebov O, Bergsagel PL, Kuehl WM. Genetic events in the pathogenesis of multiple myeloma. Best Pract Res Clin Haematol. 2007;20(4):571–596.
7. Chng, W., Dispenzieri, A., Chim, C. et al. IMWG consensus on risk stratification in multiple myeloma. Leukemia 28, 269–277 (2014).
8. Hideshima T, Mitsiades C, Tonon G, Richardson PG, Anderson KC. Understanding multiple myeloma pathogenesis in the bone marrow to identify new therapeutic targets. Nat Rev Cancer. 2007;7(8):585–598.
9. Keats JJ, Maxwell CA, Taylor BJ, et al. Overexpression of transcripts originating from the MMSET locus characterizes all t(4;14)(p16;q32)-positive multiple myeloma patients. Blood. 2005;105(10):4060–4069.
10. Brito JL, Walker B, Jenner M, et al. MMSET deregulation affects cell cycle progression and adhesion regulons in t(4;14) myeloma plasma cells. Haematologica. 2009;94(1):78–86.
11. Kuo AJ, Cheung P, Chen K, et al. NSD2 links dimethylation of histone H3 at lysine 36 to oncogenic programming. Mol Cell. 2011;44(4):609–620.
12. Pei H, Zhang L, Luo K, et al. MMSET regulates histone H4K20 methylation and 53BP1 accumulation at DNA damage sites. Nature. 2011;470(7332):124–128.
13. Popovic R, Martinez-Garcia E, Giannopoulou EG, et al. Histone methyltransferase MMSET/NSD2 alters EZH2 binding and reprograms the myeloma epigenome through global and focal changes in H3K36 and H3K27 methylation. PLoS Genet. 2014;10(9):e1004566.
14. Lhoumaud, P., Badri, S., Rodriguez-Hernaez, J. et al. NSD2 overexpression drives clustered chromatin and transcriptional changes in a subset of insulated domains. Nat Commun 10, 4843 (2019).
15. Martinez-Garcia E, Popovic R, Min D-J, et al. The MMSET histone methyl transferase switches global histone methylation and alters gene expression in t(4;14) multiple myeloma cells. Blood. 2011;117(1):211–220
16. Lauring J, Abukhdeir AM, Konishi H, et al. The multiple myeloma–associated MMSET gene contributes to cellular adhesion, clonogenic growth, and tumorigenicity. Blood. 2008;111(2):856–864.
17. Brito JLR, Walker B, Jenner M, et al. MMSET deregulation affects cell cycle progression and adhesion regulons in t(4;14) myeloma plasma cells. Haematologica. 2009;94(1):78–86.
18. Xie Z, Chooi JY, Toh SHM, et al. MMSET I acts as an oncoprotein and regulates GLO1 expression in t(4;14) multiple myeloma cells. Leukemia. 2019;33(3):739–748.
19. Garlisi CG, Uss AS, Xiao H, et al. A unique mRNA initiated within a middle intron of WHSC1/MMSET encodes a DNA binding protein that suppresses human IL-5 transcription. Am J Respir Cell Mol Biol.

2001;24(1):90–98.

20. Nishioka K, Chuikov S, Sarma K, Erdjument-Bromage H, Allis CD, Tempst P, Reinberg D. Set9, a novel histone H3 methyltransferase that facilitates transcription by precluding histone tail modifications required for heterochromatin formation. Genes Dev. 2002 Feb 15;16(4):479–89.
21. Chu L, Su MY, Maggi LB Jr, et al. Multiple myeloma-associated chromosomal translocation activates orphan snoRNA ACA11 to suppress oxidative stress. J Clin Invest. 2012;122(8):2793–2806.
22. Mirabella F, Wu P, Wardell CP, et al. MMSET is the key molecular target in t(4;14) myeloma. Blood Cancer J. 2013;3(5):e114.
23. Fingerman IM, Du HN, Briggs SD. In vitro histone methyltransferase assay. CSH Protoc. 2008 Feb 1;2008:pdb.prot4939.
24. Morey L, Helin K (2010) Polycomb group protein-mediated repression of transcription. Trends Biochem Sci 35: 323–332.
25. Feng Q, Wang H, Ng HH, Erdjument-Bromage H, Tempst P, Struhl K, Zhang Y. Methylation of H3-lysine 79 is mediated by a new family of HMTases without a SET domain. Curr Biol. 2002 Jun 25;12(12):1052–8.
26. Asangani IA, Ateeq B, Cao Q, et al. Characterization of the EZH2-MMSET histone methyltransferase regulatory axis in cancer. Mol Cell. 2013;49(1):80–93.
27. Gulati N, Béguelin W, Giulino-Roth L. Enhancer of zeste homolog 2 (EZH2) inhibitors. Leuk Lymphoma. 2018 Jul;59(7):1574–1585.
28. Page TH, Urbaniak AM, Espirito Santo AI, et al. Bruton's tyrosine kinase regulates TLR7/8-induced TNF transcription via nuclear factor-κB recruitment. Biochem Biophys Res Commun. 2018;499(2):260–266.
29. N. P. Shinners, G. Carlesso, I. Castro, K. L. Hoek, R. A. Corn, R. L. Woodland, M. L. et al. Bruton’s tyrosine kinase mediates NF-κB activation and B cell survival by B cell-activating factor receptor of the TNF-R family. The Journal of Immunology November 1, 2007, 179 (9) 6369
30. Byrd JC, Furman RR, Coutre SE, Flinn IW, Burger JA, Blum KA, Grant B, Sharman JP, Coleman M, Wierda WG, et al. Targeting BTK with ibrutinib in relapsed chronic lymphocytic leukemia. N Engl J Med. 2013;369:32–42.
31. Burger JA, Tedeschi A, Barr PM, Robak T, Owen C, Ghia P, Bairey O, Hillmen P, Bartlett NL, Li J, et al. Ibrutinib as initial therapy for patients with chronic lymphocytic leukemia. N Engl J Med. 2015;373:2425–2437.
32. Wang, M. L. et al. Targeting BTK with ibrutinib in relapsed or refractory mantle-cell lymphoma. N. Engl. J. Med. 369, 507–516 (2013).
33. Viatour P, Merville MP, Bours V, Chariot A. Phosphorylation of NF-kappaB and IkappaB proteins: implications in cancer and inflammation. Trends Biochem Sci. 2005 Jan;30(1):43–52.
34. Weber AN, Bittner Z, Liu X, Dang T-M, Radsak MP and Brunner C (2017) Bruton’s Tyrosine Kinase: An Emerging Key Player in Innate Immunity. Front. Immunol. 8:1454.

35. BTK inhibitor ibrutinib is cytotoxic to myeloma and potently enhances bortezomib and lenalidomide activities through NF-κB
36. Ibrutinib targets microRNA-21 in multiple myeloma cells by inhibiting NF-κB and STAT3
37. Murray MY, Zaitseva L, Auger MJ, et al. Ibrutinib inhibits BTK-driven NF-κB p65 activity to overcome bortezomib-resistance in multiple myeloma. Cell Cycle. 2015;14(14):2367–2375.
38. Fischle W, Wang YM, Allis CD. Histone and chromatin cross-talk. Curr Opin Cell Biol. 2003;15(2):172–183.
39. Lee JS, Smith E, Shilatifard A. The language of histone crosstalk. Cell. 2010;142(5):682–685.
40. Kim JY, Kee HJ, Choe NW, et al. Multiple-myeloma-related WHSC1/MMSET isoform RE-IIBP is a histone methyltransferase with transcriptional repression activity. Mol Cell Biol. 2008 Mar;28(6):2023–34.
41. Woo Park J, Kim KB, Kim JY, Chae YC, Jeong OS, Seo SB. RE-IIBP Methylates H3K79 and Induces MEIS1-mediated Apoptosis via H2BK120 Ubiquitination by RNF20. Sci Rep. 2015 Jul 24;5:12485.
42. Voigt P, Tee WW, Reinberg D. A double take on bivalent promoters. Genes Dev. 2013;27(12):1318–1338.
43. Chong PSY, Chooi JY, Lim JSL, Toh SHM, Tan TZ, Chng WJ. SMARCA2 Is a Novel Interactor of NSD2 and Regulates Prometastatic PTP4A3 through Chromatin Remodeling in t(4;14) Multiple Myeloma. Cancer Res. 2021 May 1;81(9):2332–2344.
44. Hendriks RW, Yuvaraj S, Kil LP. Targeting Bruton's tyrosine kinase in B cell malignancies. Nat Rev Cancer. 2014 Apr;14(4):219–32.
45. Bohnhorst, J., Rasmussen, T., Moen, S. et al. Toll-like receptors mediate proliferation and survival of multiple myeloma cells. Leukemia 20, 1138–1144 (2006).
46. Chong PSY, Zhou J, Lim JSL, Hee YT, Chooi JY, Chung TH, Tan ZT, Zeng Q, Waller DD, Sebag M, Chng WJ. IL6 Promotes a STAT3-PRL3 Feedforward Loop via SHP2 Repression in Multiple Myeloma. Cancer Res. 2019 Sep 15;79(18):4679–4688
47. Chong PSY, Chng WJ, de Mel S. STAT3: A Promising Therapeutic Target in Multiple Myeloma. Cancers (Basel). 2019;11(5):731.
48. Harmer D, Falank C, Reagan MR. Interleukin-6 Interweaves the Bone Marrow Microenvironment, Bone Loss, and Multiple Myeloma. Front Endocrinol (Lausanne). 2019 Jan 8;9:788.
49. Huang DW, Sherman BT, Lempicki RA. Systematic and integrative analysis of large gene lists using DAVID Bioinformatics Resources. Nature Protoc. 2009;4(1):44–57.

Figures

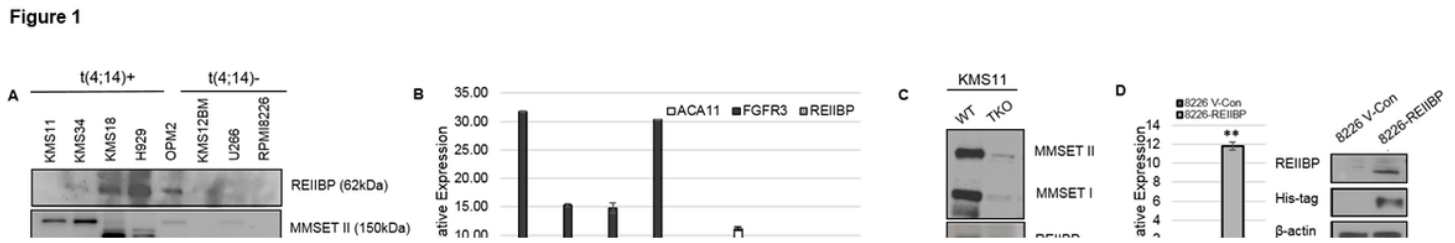

Figure 1

REIIBP is oncogenic and overexpressed in t(4;14) cells. (A) Western blotting to determine the endogenous expression of MMSET I, II and REIIBP in a panel of human myeloma cell lines. GAPDH was used as loading control. (B) qRT-PCR analysis of ACA11, FGFR3 and REIIBP in a panel of human myeloma cell lines. GAPDH was used as for normalization. (C) mRNA and protein were extracted from isogenic cells, KMS11-WT and KMS11-TKO (translocation knockout) cells to determine the expression of MMSET I, II and REIIBP. (D) Overexpression of REIIBP in RPMI8226 cells was determined using qRT-PCR and Western blotting. REIIBP expression vector contained His-tag and β-actin was used as loading control. (E) 10 million RPMI8226 V-Con or REIIBP cells (left) or H929 (right) were lysed to extract the nuclear (NER) and cytoplasmic (CER) protein fractions. Minimal cross-contamination was confirmed with nuclear marker lamin A and cytoplasmic marker α-tubulin. MMSET I and II were found in the nucleus as previously reported. (F) Cell viability was determined over 72 hours in RPMI8226 control and REIIBP-overexpressing cells and normalized against 0 hours. (G) Colony-forming assay was performed to determine the long-term viability of RPMI8226 control and REIIBP-overexpressing cells over two weeks and the number of colonies was plotted. (H) Cell cycle analysis of RPMI8226 control and REIIBP-overexpressing cells were measured using flow cytometry and the percentage of cells in G1, S or G2/M were indicated. Experiments were performed with three biological repeats and a representative experiment was shown. Asterisks represent significant differences (*, $P < 0.05$; **, $P < 0.01$, Student t test).

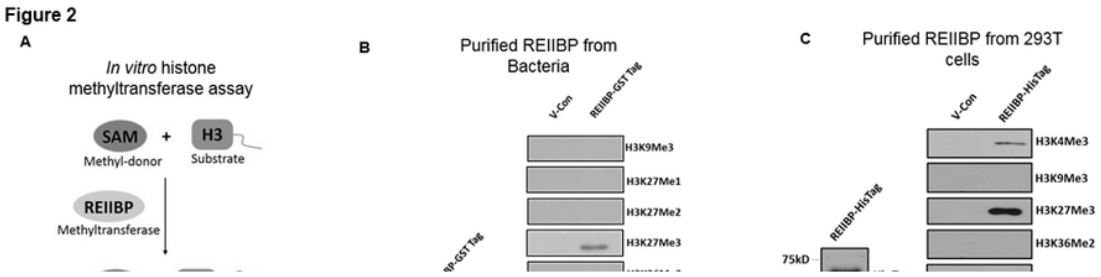

Figure 2

***In vitro* histone methyltransferase assay to confirm that REIIBP has a direct effect on histone methylation.** (A) Diagrammatic representation of the *in vitro* methylation assay with S-adenosyl-L-methionine (SAM) was shown. Purified REIIBP methyltransferase from (B) E.coli or (C) 293T cells was added to SAM and H3 substrate in PKMT buffer. Western blotting was performed with the indicated antibodies. (D) H3K27 methyltransferase activity assay was performed using increasing amount of nuclear extract from RPMI8226-Vector Control (V-Con) or RPMI8226-REIIBP cells and readings were taken at 450 nm. (E) H3K4 methyltransferase activity assay was performed using increasing amount of nuclear extract from RPMI8226-Vector Control (V-Con) or RPMI8226-REIIBP cells and readings were taken at 450 nm. Experiments were performed with three biological repeats and a representative experiment was shown. Asterisks represent significant differences (*, $P < 0.05$; **, $P < 0.01$, Student t test).

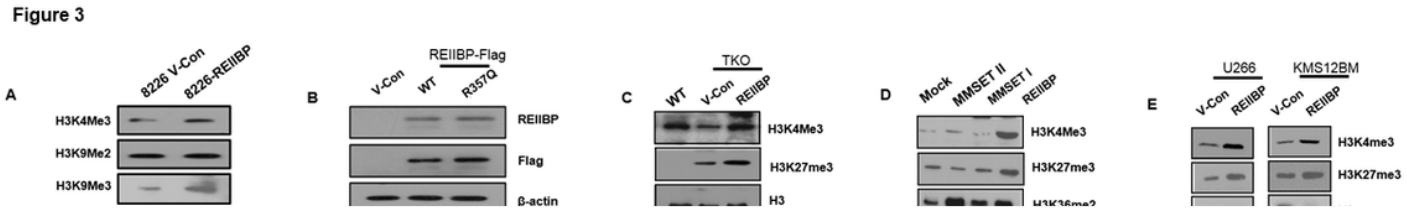

Figure 3

REIIBP alters global levels of histone methylation. (A) 50μg of protein lysate from RPMI8226-Vector Control (V-Con) and RPMI8226-REIIBP cells were used for Western Blotting with the indicated antibodies. H3 is the loading control. (B) Control vector, wild-type REIIBP and R357Q mutant REIIBP were transiently transfected into RPMI8226 cells and 50μg of protein lysate were used for Western Blotting with the indicated antibodies. H3 and β-actin are the loading control. (C) KMS11 and KMS11-TKO (translocation knockout) cells transiently transfected with control vector or wild-type REIIBP were used for Western Blotting with the indicated antibodies. H3 and β-actin are the loading control for nuclear and total extract. (D) RPMI8226 cells were transfected with MMSET I, MMSET II and REIIBP expression vectors and Western Blotting with the indicated antibodies. H3 and β-actin are the loading control for nuclear and total extract. (E) U266 and KMS12BM were transiently transfected with REIIBP expression vector from Supplementary Figure 1C and used to probe for histone marks. H3 is the loading control.

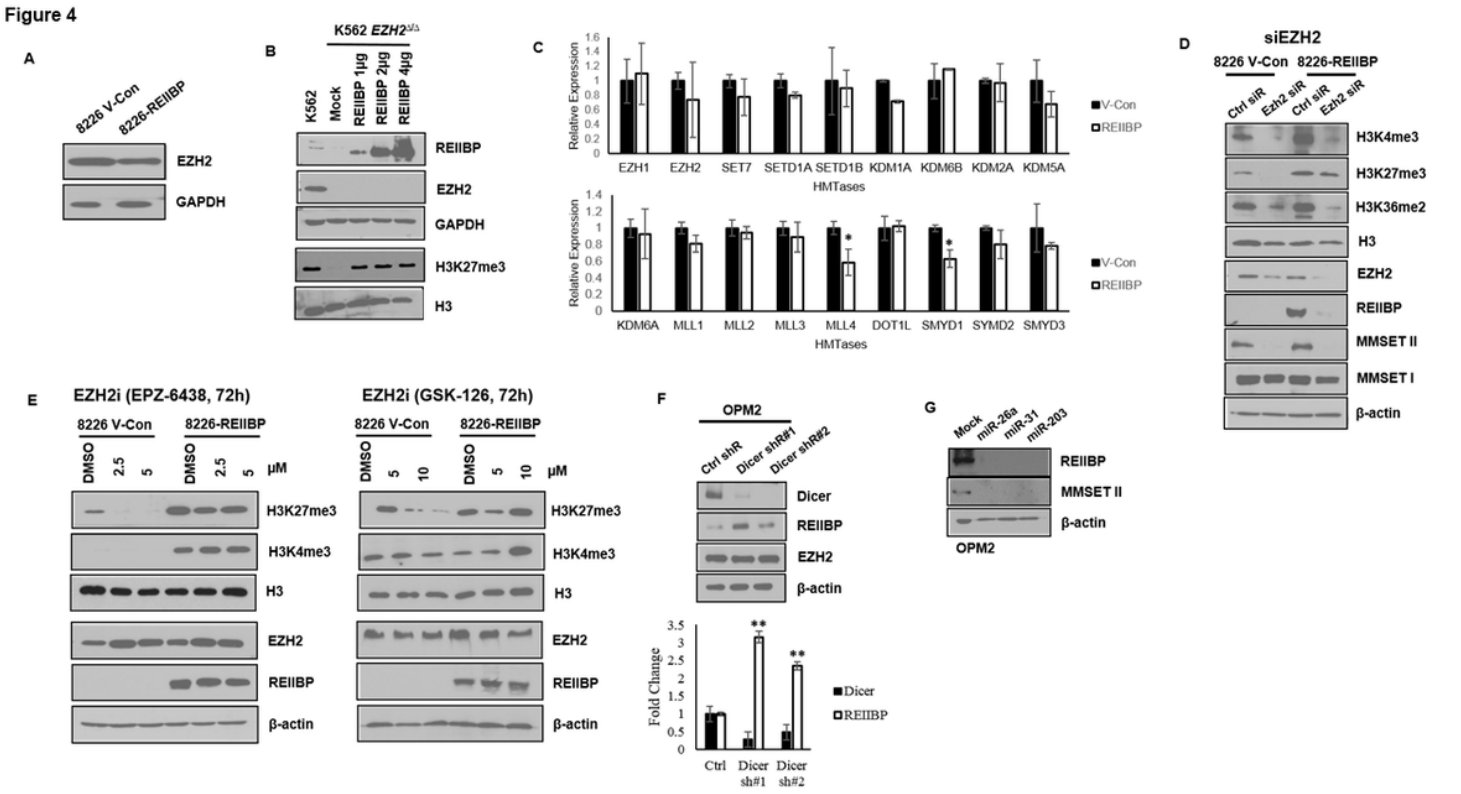

Figure 4

REIIBP regulates H3K27me3 independent of EZH2. (A) 50μg of protein lysate from RPMI8226-Vector Control (V-Con) and RPMI8226-REIIBP cells were used to check for EZH2 levels. GAPDH is the loading control. (B) K562 EZH2$^{\Delta/\Delta}$ cells were transiently transfected with increasing amounts of REIIBP plasmid and protein were extracted at 48 hrs to determine the levels of H3K27me3. GAPDH and H3 are the loading controls. (C) Gene expression of a panel of histone methyltransferases and demethylases were determined in RPMI8226-Vector Control (V-Con) and RPMI8226-REIIBP cells. GAPDH was used for normalization. (D) RPMI8226-Vector Control (V-Con) and RPMI8226-REIIBP cells were transiently transfected with control or EZH2 siRNA (100 nM) and protein harvested at 48 hours for Western Blotting with the respective antibodies. H3 and β-actin are the loading control for nuclear and total extract. (E) RPMI8226-Vector Control (V-Con) and RPMI8226-REIIBP cells were treated with two EZH2 inhibitors, EPZ-6438 and GSK-126, for 72 hours before protein was harvested for Western Blotting. H3 and β-actin are the loading control for nuclear and total extract. (F) 1 x 10^6 OPM2 cells were transiently transfected with 2μg scrambled shRNA, Dicer shRNA #1 or #2 for 48 hours and protein lysate was harvested. Western Blotting was performed with the indicated antibodies. β-actin is the loading control. Transfection for 24 hours was harvested for mRNA and shown as fold change relative to scrambled shRNA control. (G) OPM2 cells were transiently transfected with 75nM of miRNA-26, miRNA-31 or miRNA-203 for 48 hours and the protein levels of REIIBP and MMSET II were determined. Experiments were performed with three biological repeats and a representative experiment was shown. Asterisks represent significant differences (*, $P < 0.05$; **, $P < 0.01$, Student t test).

Figure 5

Global transcriptional changes in REIIBP-overexpressing cells. (A) Heat map of Log Fold-Change cut-off of 1.6 were shown. See Supplementary Table 1 for microarray data. (B) Up- and down-regulated genes were plotted as a pie chart. (C) Functional annotation clustering was performed using DAVID Bioinformatics Resources[49] with the DEGs. The processes with the top three enrichment scores are presented. The x-axis represents the number of genes, while the y-axis represents the ontology categories. (D) RPMI8226-Vector Control (V-Con) and RPMI8226-REIIBP cells were used to check the mRNA levels of five upregulated genes, *CYBB, TLR7, FAIM3, BTK* and *PDIA2*. (E) RPMI8226-Vector Control (V-Con) and RPMI8226-REIIBP cells were used to determine the protein levels of TLR7 and BTK. β-actin is the loading control. (F) Survival analysis using Cox regression & Kaplan-Meier curves were performed on TLR7 and BTK in the CoMMpass dataset. (G) The correlation between REIIBP and BTK in CoMMpass dataset was performed by first assigning REIIBP out of 31 registered MMSET transcripts. Correlation between REIIBP and BTK is significant in MMSET group (points marked in yellow, regression results represented in red) in the background of overall scatterplot. Overall regression between REIIBP and TLR7 is shown in gray. Asterisks represent significant differences (*, $P < 0.05$; Student t test).

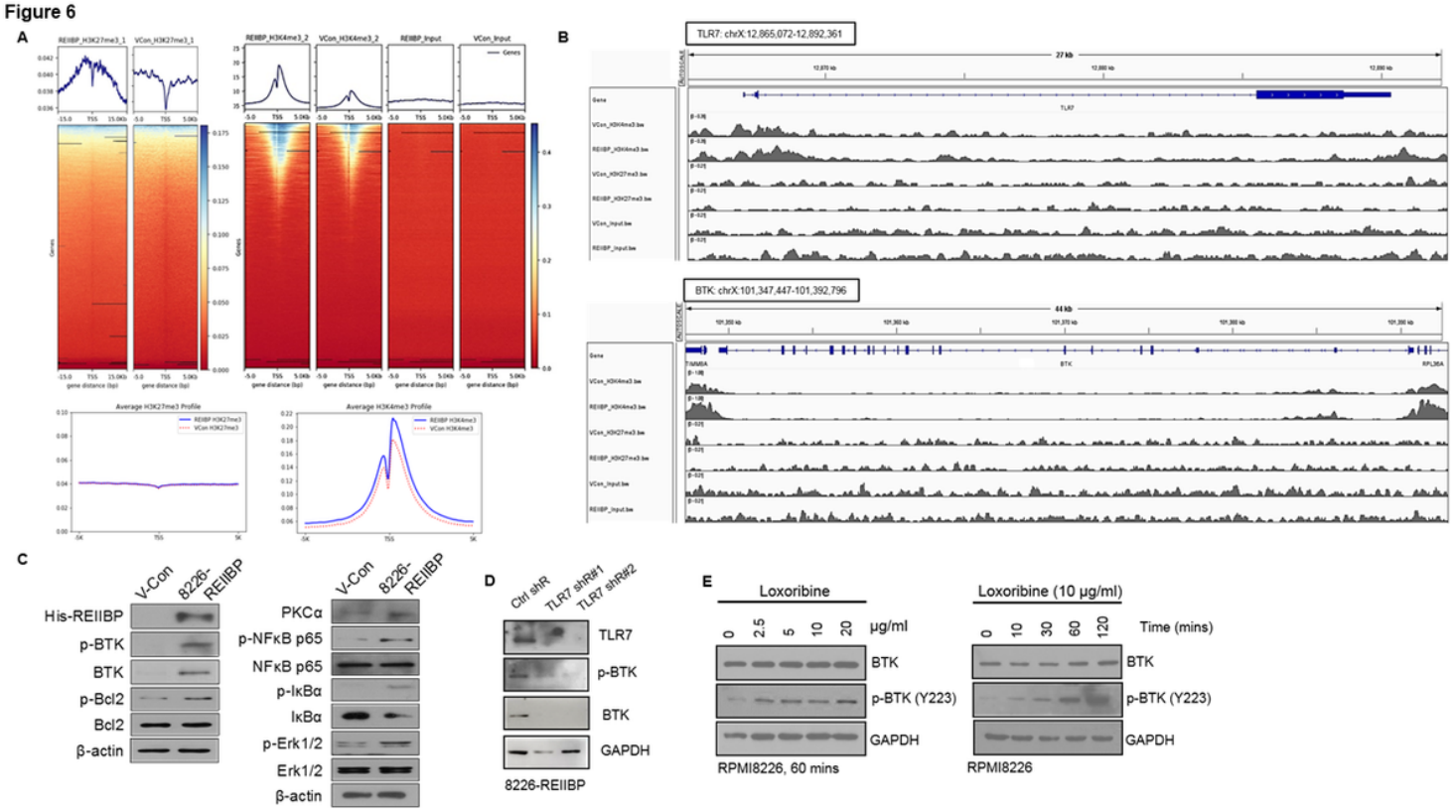

Figure 6

REIIBP activates BTK and its downstream targets in a TLR7-dependent manner. (A) Heatmap and average H3K4me3 and H3K27me3 profile enrichment on genomic loci near TSS from three replicates of ChIP-seq analysis was shown. DNA input and mouse IgG were used as controls. Raw ChIP-seq data is publicly available as GSE198026. (B) Integrative Genomics Viewer (IGV) browser representative gene tracks of TLR7 (top) and BTK (bottom) were shown for H3K4me3 and H3K27me3 histone marks in RPMI8226-Vector Control (V-Con) and RPMI8226-REIIBP cells. (C) 50µg of protein lysate from RPMI8226-Vector Control (V-Con) and RPMI8226-REIIBP cells were used with the indicated antibodies. β-actin is the loading control. (D) RPMI8226-REIIBP cells were transiently transfected with two TLR7-targeting shRNAs and protein harvested 48 hours post-transfection. Western Blotting was performed with the indicated antibodies. GAPDH is the loading control. (E) RPMI8226 cells were treated with increasing concentration of loxoribine for 60 mins (left) or increasing duration at fixed concentration of 10 µg/ml (right). Phospho-BTK and total BTK levels were determined using Western Blotting and GAPDH is the loading control.

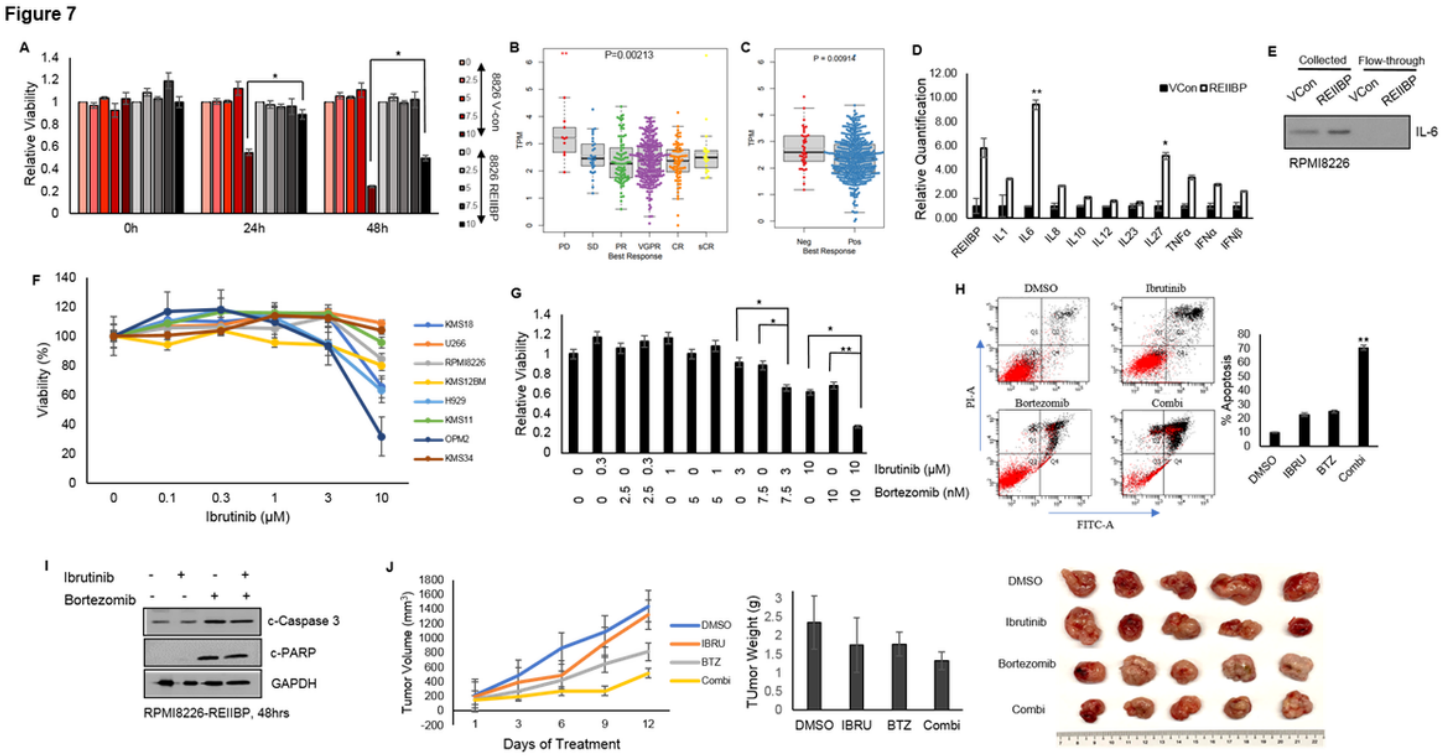

Figure 7

Inhibitory effects of combining Ibrutinib with Bortezomib. (A) RPMI8226-Vector Control (V-Con) and RPMI8226-REIIBP cells were treated with increasing concentrations of Bortezomib (0, 2.5, 5, 7.5, 10nM) and viability was determined at 24 and 48 hours using CTG assay. Viability was normalized against 0nM. Experiments were performed with three biological repeats and a representative experiment was shown.

(B) REIIBP expression by 6-level best response to Bortezomib without t(4;14) cases in CoMMpass dataset. PD (progressive disease: 1.6%, 12/745), SD (stable disease: 6.3%, 47/745), PR (partial response:17.4%, 130/745), VGPR (very good partial response: 51.9%, 387/745), CR (complete response: 18.7%,139/745), sCR (stringent complete response: 4%, 30/745). (C) REIIBP expression by 2-level best response to Bortezomib without t(4;14) cases in CoMMpass dataset. Negative (PD + SD: 7.9%, 59/745) and Positive (PR + VGPR + CR + sCR: 92.1%, 686/745). (D) The expression of various cytokines and chemokines were determined in RPMI8226-Vector Control (V-Con) and RPMI8226-REIIBP cells. GAPDH was used for normalization. (E) IL-6 in the cell culture supernatant was collected from filter unit and flow-through, and measured by Western Blotting in RPMI8226-Vector Control (V-Con) and RPMI8226-REIIBP cells. (F) Panel of myeloma cell lines were treated with increasing concentrations of Ibrutinib for 48 hours and viability was plotted. (G) RPMI8226-REIIBP cells were treated with single or combination of fixed-ratio concentrations of Ibrutinib and Bortezomib and viability was determined at 48 hours. Experiments were performed with three biological repeats and a representative experiment was shown. (H) RPMI8226-REIIBP cells treated with DMSO, 10 μM Ibrutinib, 10 nM Bortezomib or combination were subjected to Annexin V-PI flow cytometry to determine apoptosis. (I) The expression of cleaved caspase-3 and cleaved PARP is determined by Western Blotting in RPMI8226-REIIBP cells treated with DMSO, 10 μM Ibrutinib, 10 nM Bortezomib or combination after 48 hours. GAPDH is the loading control. (J) Xenografts of RPMI8226-REIIBP (5 million cells) were allowed to grow for three weeks until desired size, and treatment with 1% DMSO, 20 mg/kg Ibrutinib, 0.4 mg/kg Bortezomib or combination proceeded for 2 weeks. Tumors were harvested and weighed in grams. Harvested tumors were photographed. Asterisks represent significant differences (*, $P < 0.05$; **, $P < 0.01$, Student t test).

Supplementary Files

This is a list of supplementary files associated with this preprint. Click to download.

- REIIBPSupplementaryMaterialsandMethods.docx
- SupplementaryTable1.8226RelIBPvsVCFC1.3.xlsx